A comprehensive heat generation study of lithium titanate oxide-based lithium-ion batteries

A comprehensive heat generation study of lithium titanate oxide-based lithium-ion batteries

Seyed Saeed Madani[1,2 *], Erik Schaltz[2], Søren Knudsen Kær[2] and Carlos Ziebert[1]

[1] Institute of Applied Materials-Applied Materials Physics, Karlsruhe Institute of Technology, Hermann-von-Helmholtz-Platz 1, 76344 Eggenstein-Leopoldshafen, Germany
[2] Department of Energy Technology, Aalborg University, DK-9220 Aalborg, Denmark
[*] seyed.madani@kit.edu

Abstract. A precise interpretation of lithium-ion battery (LIB) heat generation is indispensable to the advancement and accomplishment of thermal management systems for different applications of LIB, including electric vehicles. The internal resistance of a lithium titanate oxide (LTO)-based LIB was determined at different state of charge (SOC) levels and current rates to understand the relationship between internal resistance and heat generation. Random and different pulse discharge current step durations were applied to consider the effect of different SOC interval levels on heat generation. The total generated heat was measured for different discharge rates and operating temperatures in a Netzsch IBC 284 calorimeter. It was seen that a 6.7% SOC decrease at high SOC levels corresponds to 0.377 Wh, 0.728 Wh, and 1.002 Wh heat generation for 26A, 52A, and 78A step discharge, both at 20 °C and 30 °C. However, a 1.85% SOC decrease at medium SOC levels corresponds already to 0.57 Wh, 0.76 Wh, and 0.62 Wh heat generation. It can be inferred that the impact of SOC level on heat generation for this cell is more prominent at a lower than at a higher SOC.

1. Introduction

Quantifying localized heat loss within a lithium-ion cell is a challenging research area due to unpredictability regarding cells' inner architecture, active materials, and thermal properties [1]. Some researchers used a calorimeter. Previous investigations employed tiny cells and samples to accomplish tests through different calorimeters [2-4]. Only a few researchers investigated commercial pouch cells [5]. Experimental and simulation investigations have been accomplished to investigate the impact of heat generation of LIB on temperature distribution. Outcomes demonstrate that the battery's local temperature is the largest at the positive and negative terminals at the discharge end, attributable to the more significant current density at these positions [6-8]. A thermal model was investigated by incorporating a different approach. The effect of coolant flow configurations on temperature distributions was studied to consider other aspects of the model. Besides, the thermal performance was evaluated for various thermal management strategies [9].

In the previous investigations of the authors [10-14], various experimental research has been accomplished on the thermal performances of LIB, and their heat generation was studied. In addition, the effect of the current rate, state of charge (SOC), and temperature on heat generation at different current rates and operational temperatures was determined.

In [10,11], the lithium-ion battery was subjected to different charge and discharge experiments under working temperatures of 30 °C, 40 °C, and 50 °C employing the experimental methodology explained in [10-14]. Sixteen charge and discharge cycles ranging from 13 A to 104 A were applied to the lithium titanate oxide (LTO) battery. Numerous experiments were accomplished at different

working temperatures, including 30 °C, 40 °C, and 50 °C. A trend almost identical to the one seen at working temperatures of 30 °C was seen for the heat generation in working temperatures of 40 °C and 50 °C. The heat losses during the 8 C discharge cycle for working temperatures 50 °C, 30 °C, and 40 °C were 7.3, 8, and 8 times bigger than the 1C cycle. The outcomes demonstrate that the heat loss for discharge condition began with 6952 J, 5511 J, and 3550 J at 50 °C, 40 °C, and 30 °C during the 1C discharge cycle and reached 50852 J, 43302 J, and 28138 J during 8C discharge cycle. When a specific loading pattern was applied, the sum of total heat generations during 16 charging and discharging cycles was different under dissimilar working conditions. As a result, at a working temperature of 40 °C, the cell undergoes a 60% increase in the total heat generation compared to a working temperature of 30 °C measured under identical conditions. The cell at a working temperature of 50 °C produced 32% and 112% more heat than working temperatures of 40 °C and 30 °C, respectively. Nevertheless, the percentage growth in total heat generation due to a change in working temperature from 30 °C to 40 °C was more significant than the ratios achieved due to a change in working temperature from 40 °C to 50 °C. Accordingly, working temperatures of 30 °C were considered more efficient and better suited than those of 40 °C and 50 °C [10-14].

The efficiency throughout charging began with 93.86% for 1C and decreased to 49.19% for 8.5C. The efficiency throughout discharging began with 93.22 % for 1C and declined to 68.67% for 8C. Heat loss throughout discharging cycles showed nearly an identical behaviour as for the charging cycles, which was a growing pattern from 1C to 8C. The heat generation began with 8424 J for 1C throughout the discharge cycle and attained 40,100 J for the 8C cycle. The most effective rising rate was from the 7C cycle to the 7.5C cycle (a growth of 11.1%). The smallest increase was from 7.5C cycle to 8C cycle, which was approximately 100 J. A five-fold increase was seen in heat generation from 1C cycle to 8C cycle during discharge. The alteration between discharge and charge heat losses was approximately identical for all current rates at 50 °C and 40 °C. On the contrary, this alteration experienced various oscillations at 30 °C with the most considerable quantity in the 8C cycle [10-14].

The charge efficiency for 40 °C declined by approximately 27%, even though this percentage during discharge was approximately 35%. The heat losses during the 8C charging cycle for 50 °C, 40 °C, and 30 °C were 8.4, 12.5, and 8.5 times bigger than for the 1C cycle. The total heat generation of the cells during the 91 A discharge cycle was approximately 1100 J more than the total heat generation during the 91 A charge cycle in working temperatures of 30 °C. It was observed that notwithstanding the heat generation throughout 26 A charging cycle and discharging cycle are almost identical in working temperatures of 30 °C, approximately an additional 3500 J has to be transferred from the cell at the end of the discharge cycle, assuming its temperature should be maintained at working temperatures of 40 °C. A considerable rise could be seen in the cell's heat generation as the working temperature increased from 30 °C to 50 °C. Those mentioned above could demonstrate a considerable decrease in cell performance and unsatisfactory electrochemical efficiency at significant temperatures. In the current rates range of 13 A to 104 A, the average heat flux quantified for the working temperature of 50 °C was more significant than for the working temperatures of 30 °C and 40 °C. Heat loss following discharge and charge cycles contributes considerably to the cells' entire heat generation. The average percentages of contribution for discharge and charge cycles ranging from 13 A to 104 A were 79.3%,77.6%, and 79.3% of the entire heat generation at 30 °C, 40 °C, and 50 °C. Accordingly, the heat of mixing cannot be disregarded. It was concluded that the ratio of heat loss to electrical energy lost attributable to alteration was not on the same order of magnitude for all charge and discharge cycles [10-14].

In another work [12], numerous experiments were accomplished at a working temperature of 20 °C. Thirty-one charge and discharge cycles ranging from 13 A to 110 A were applied to the same LTO-based LIB. The thermal efficiency throughout charging was smaller than that for discharging, except for 13 A, 19.5 A, and 26 A, which was more significant. The difference between charge and discharge efficiencies raised at bigger current rates. This discrepancy was most significant at 97.5 A. It was seen that the heat loss during charging was lower than that during discharging, excluding 104 A and 97.5 A, where it was bigger. The difference between charge and discharge heat losses stayed nearly identical for all current rates. The discrepancy was most significant at 19.5 A. The heat loss for discharging and charging cycles was determined to be 34,100 J and 35,793 J for the 8C cycle and 8.5C

cycle, respectively. The average quantity of heat flux at 20 °C and 110.5 A was 9.5 W. This value is 19 times bigger than at 3 A, which is 0.5 W. The efficiency throughout charging began with 97.69%, 96.92%, and 95.24% for 1C and attained 82.8%, 70.36%, and 62.1% for 8C. The heat loss throughout charging began with 2697J, 3264J, and 5744J for 1C and attained 22926J, 40839J, and 48185J for 8C [10-14].

In [13], a thermal model was derived from the computation of the heat loss from the entropic heat coefficient and the internal resistance measurements. Calorimetry data were compared with estimates from the thermal model. The experiment agreed well with the modelling results, which were gained at different current rates. The modelling was validated by comparing the exploratory consequences with the modelling discharge figures at various discharge rates and environmental temperatures. A medium heat capacity was assumed for the cell in the time-conditional and unsteady condition simulation. Experimental investigations were restricted to surface temperatures integrated with heat dissipation's thermal or analytical modelling to achieve cell temperatures and determine the total heat loss of the cell [12]. The surface fitting and voltage alterations for 50%, 60%, 70%, and 80% SOC were determined throughout the thermal process. The slope of these surfaces corresponded to the average cell voltage, which was determined as a function of the SOC. Besides, the cells' entropic heat coefficient was calculated as a function of the SOC. The investigated cell's internal resistance was determined using the hybrid pulse procedure. Heat generation and efficiency of the cell as a function of the SOC were determined. It was found that the heat generation showed an almost diminishing pattern from 10 % to 90% SOC for all current rates. The cells' potential and reversible entropic heat showed a declining pattern towards a significant SOC [10-14].

Heat generation at different current rates of charge and discharge cycles was separated into four sections corresponding to the operational temperature of the LIB. It was concluded that between 20 °C and 50 °C, heat generation for 13 A and 104 A charge was in the range of 3000-7000 J and 23000-48000 J, respectively. The difference between charge and discharge heat generations was calculated. It was shown that the variation tendency of heat generation differences at various temperatures was different. This variation reaches its minimum value at higher current rates, such as 78 A and 91 A, for 20 °C, but it reaches its maximum value at 40 °C and 78 A. It can be concluded that heat generation differences at various current rates and temperatures do not follow a regular pattern. Thermal characterization of the cell revealed that the surface temperature distributions of the cell raised with the charge and discharge rate (1C, 2C, 3C, to 10C) and operational temperature (20°C, 30°C, 40°C, 50°C). It was seen that 50°C and 30°C cases created the highest and lowest heat generation [10-14].

Notwithstanding, the heat generation decreased from 20 °C to 30 °C. The heat generation dropped from 20 °C to 40 °C except for high current rates, including 104 A, 91 A, and 78 A. This phenomenon was not observed in the literature for the investigated cell type. It may be attributable to internal cell resistance, polarization losses, phase change mechanisms, and overpotential [10-14].

As was described comprehensively in their previous investigations [10-14], the authors did not perform thermal characterizations of the LTO-based cells that focused on periodic charge and discharge pulses. In addition, to the author's knowledge, all other investigations in the literature [15-32] were limited to the heat generation measurement of lithium-ion batteries during constant current charge and discharged complete cycles. Accordingly, the present work aims to measure the heat generation rates of LTO-based lithium-ion cells for different intervals of SOC levels.

The heat generation of LIB is a challenging task because of the complex electrochemical reactions occurring and their dependence on different parameters. The overpotential represents system irreversibility and is considered a discrepancy between the cells' terminal voltage and its theoretical open circuit potential. Heat is generated that can be attributed to transport resistances and electrochemical reactions inside a LIB [22,23].

Different methods were used in the literature for thermal behaviour and heat generation determination of LIB [24-34]. Most of them were restricted to small coin types and small cylindrical batteries. These batteries are not appropriate for large-scale applications, including electric vehicles. Besides, almost all previous research employed low discharge rates, not representing the electric cars' electrical demands. The aforementioned shows the necessity of new research approaches for superior comprehension of LTO-based cells' heat generation mechanisms. LTO-based cells are characterized

by significant power capability throughout discharging and charging, high safety, good thermal stability, and a long lifetime, which is generally attributable to the small operating voltage. LTO-based LIB has become a valuable new energy source for certain electric vehicles, accompanied by grid power storage systems and portable electronic devices. LTO is presently one of the leading nominees as anode material for the lithium-ion battery as a consequence of its lifetime and safety properties [35].

There are lithium titanate nanocrystals on the anode surface of LTO-based lithium-ion batteries. The aforementioned makes them charge faster than other LIBs. They have several features, including lifetime and safety properties, making them an appreciable and promising technology for different applications such as e-mobility and grid storage. LTO-based lithium-ion batteries with different cathode materials were assessed and designed for realistic applications [35,36].

Consequently, in the accessible literature, there was a lack of articles that systematically analyzed the LTO-based LIB heat generation focusing on random and periodic charge/discharge current pulses. The aforementioned is closer to the actual application of lithium-ion batteries, especially in electric vehicles. Preceding investigations have mainly concentrated on studying LIB packs' thermal performance. Notwithstanding, an isothermal battery calorimeter was rarely employed as a proper and precise instrument for quantifying heat generation inside LIB.

Many studies have been accomplished on the thermal analysis of lithium-ion cells, but only a few employed an experimental calorimetry procedure to determine LIB heat generation. In most of the previous investigations, the amount of heat generation was only calculated. In the present work, a Netzsch IBC 284 isothermal battery calorimeter was employed to precisely determine heat generation. In addition, internal resistance and open-circuit voltage were determined to assist in understanding the thermal behaviour and heat generation of LTO-based cells. The results' originality and novelty are that an isothermal battery calorimeter was used to study the LTO-based cells' thermal behaviour with a particular focus on periodic charge and discharge pulses.

Because LTO-based cells are still quite a new chemistry, their thermal characteristics and behaviour are not entirely understood. The current work might assist in establishing a thermal model of the cell and employing it unaccompanied by extensive comprehension of electrochemistry. Furthermore, the priority was on employing straightforward and uncomplicated methodologies for parameter determination.

2. Experimental

2.1. Cell description

The lithium-ion battery cells employed in this study are 13 Ah high-power lithium titanate oxide-based lithium-ion battery cells with $LiNi_xMn_yCo_zO_2$ (NMC) on the cathode side and $Li_4Ti_5O_{12}$ (LTO) on the anode side. The minimum and maximum voltage are 1.5V and 2.9V, respectively. The nominal voltage is 2.26 V. Characteristics of the LTO Li-ion battery based is demonstrated in Table 1.

Table 1. Characteristics of LTO Li-ion battery based.

Property	Value
Minimum voltage	1.5 V
Maximum charging voltage	2.9 V
Nominal voltage	2.26 V
Nominal capacity	13 Ah
Maximum discharge current	130 A
Maximum charge current	130 A
Anode	Li4Ti5O12
Cathode	Li(NixMnyCoz)O2
Calendar life	25 years

2.2. Setup of the experiments

This research employed the isothermal IBC284 calorimeter (Netzsch) to characterize the heat loss related to constant current discharge (CCD) and constant current charge (CCC) procedures. Four different current profiles were applied with random and periodic current pulses. Therefore, ten different step time durations were applied for SOC determination. The cell under investigation was inserted into the calorimeter chamber, their terminals were connected to a Maccor battery cycler, and four thermocouples T1-T4 were attached to the cell, as illustrated in Figure 1.

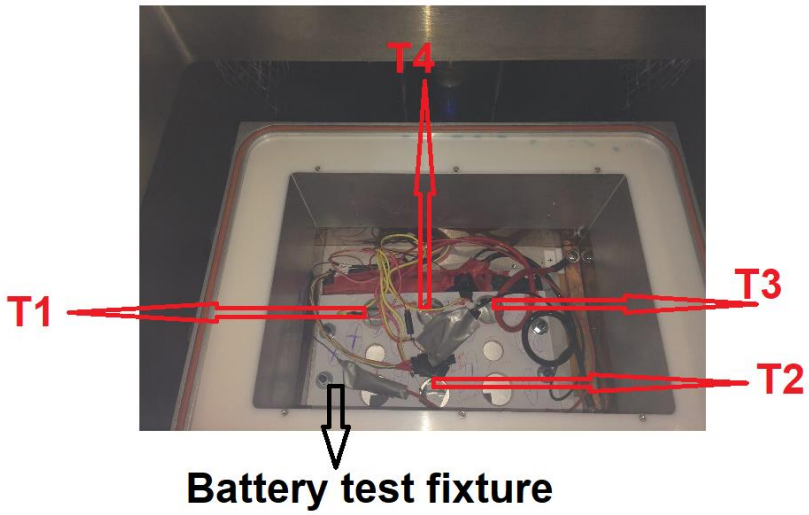

Figure 1. Setup of the battery cell and thermocouples inside the calorimeter chamber.

Figure 2 shows the experimental system setup for determining heat generation and internal resistance. Figure 2(a) depicts the calorimeter system setup, while Figure 2(b) explains the connection to the Maccor cycler.

The maximum discharge and charge current was 130 A. Attributable to safety concerns, accompanied by the simple connection of the voltage cables and power, the cell was examined in the laboratory by installing it on a fixture, which prevents volume alteration. The volume expansion is because of working with high temperatures and high current rates.

This research employed calorimetry to characterize the heat loss related to different discharge and charge profiles. The cell thermal analysis was accomplished, employing Proteus Analysis Software and MATLAB. Consequently, calibration was done before each experiment to achieve higher accuracy. Besides, the thermocouples heat flux sensors were used in this research.

The isothermal battery calorimeter is a robust instrument fabricated for correctly determining heat flux produced by lithium-ion batteries while being charged or discharged under the experiential situation. The isothermal battery calorimeter unit contains one empty cabinet (650 lbs./300kg). The thermal fluid appends 250 lbs./114 kg of extra weight, and the computer links to the instrument cabinet through two USB 2.0 cables. Multiple procedures of commercially accessible temperature control were used for the experiments. Dissimilar and independent loading were exerted on the cell. Besides, comprehensive characterization tests were done for these cells.

To estimate the heat generation of the LTO-based cell with an isothermal battery calorimeter, the cell and the calorimeter chamber need to reach a specified steady-state temperature before and after the cell cycle. The calorimeter and the cell with the expected state of charge are taken to the specified temperature while the cell is in the isothermal battery calorimeter. It takes about six hours for the cell and the isothermal battery calorimeter chamber to reach thermal equilibrium. The aforementioned is mainly attributable to the considerable thermal mass of the isothermal battery calorimeter. Afterwards, a specified load is applied to the cell with the Maccor battery cycler. Afterwards, the isothermal battery calorimeter needs another six hours for the temperature to equilibrate.

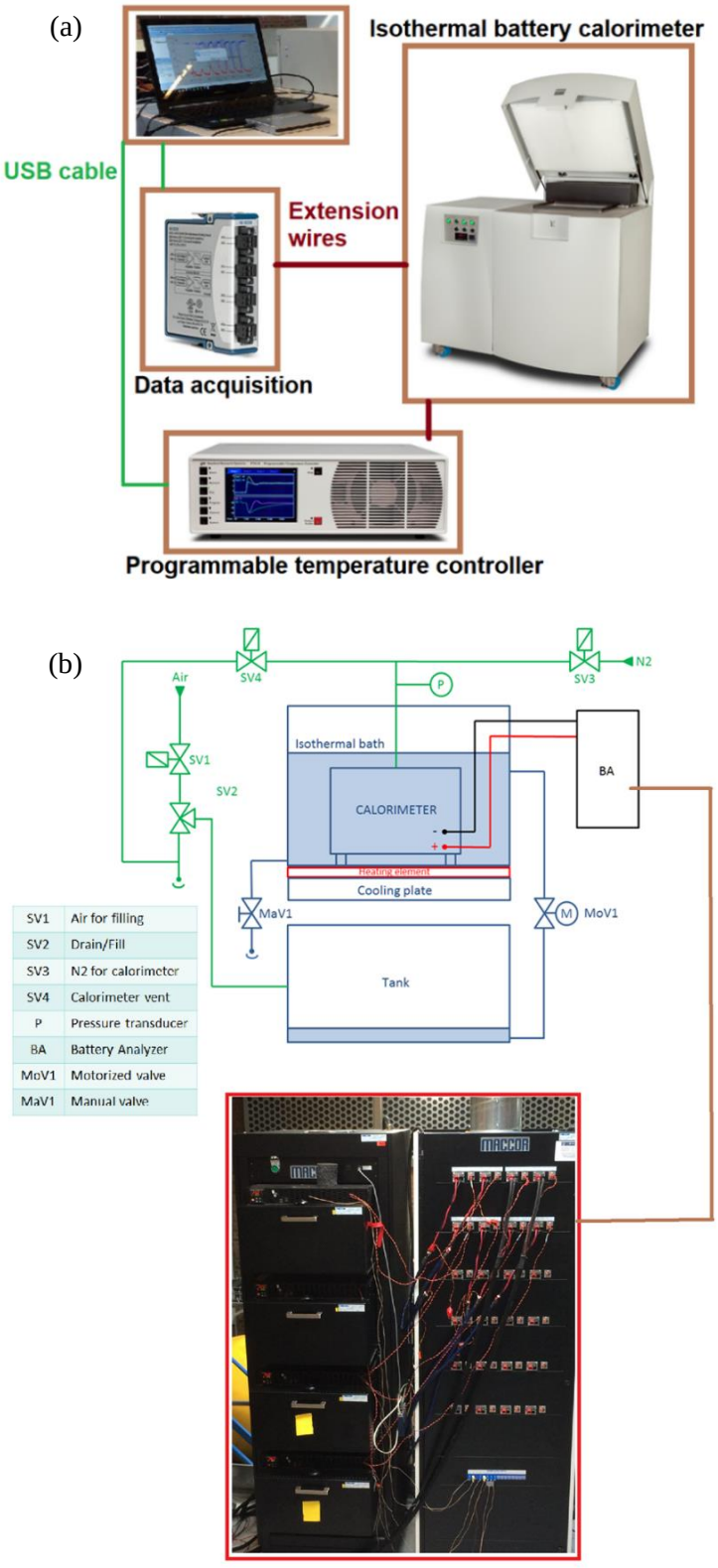

Figure 2. Experimental facilities for determination of LTO-based cell heat generation and internal resistance (a) Schematics of the experimental setup, (b) Connecting the battery cycler.

2.3. Procedures for the experiments

In the present investigation, the cell was discharged to the selected state of charge level with different current rates. Once the selected state of charge level was obtained, the cell was left to stabilize. The experiments demonstrated that this stabilization time was approximately the same for different state of charge levels. Table 2 describes the procedures for the experiments.

Table 2. The procedures for the experiments. (HG: heat generation).

Step 26 A discharge 20 °C	Step 52 A discharge 20 °C	Step 78 A discharge 20 °C	Cut off voltage	State of charge	HG: Step 26 A discharge 20 °C	HG: Step 52 A discharge 20 °C	HG: Step 78 A discharge 20 °C	HG: Step 26 A discharge 30 °C
3.25 A-CCC	3.25 A-CCC	3.25 A-CCC	2.132	76.14				0
3.25 A-CCD	3.25 A-CCD	3.25 A-CCD	2.8	100				
3.25 A-CCC	3.25 A-CCC	3.25 A-CCC	1.5	0	1.863	1.925	1.96	0.7461
3.25 A-CCD	3.25 A-CCD	3.25 A-CCD	2.8	100				
3.25 A-CCD	3.25 A-CCD	3.25 A-CCD	2.474	74.92				
26 A-PD	52 A-PD	78 A-PD	2.387	68.23	0.377	0.728	1.002	0.2249
26 A-PD	52 A-PD	78 A-PD	2.315	62.69	0.390	0.730	1.012	0.2210
26 A-PD	52 A-PD	78 A-PD	2.262	58.61	0.386	0.708	1.017	0.2290
26 A-PD	52 A-PD	78 A-PD	2.224	55.69	0.401	0.726	1.005	0.2310
26 A-PD	52 A-PD	78 A-PD	2.198	53.69	0.400	0.776	1.064	0.2290
26 A-PD	52 A-PD	78 A-PD	2.176	52.00	0.413	0.749	1.077	0.2280
26 A-PD	52 A-PD	78 A-PD	2.153	50.23	0.429	0.785	1.090	0.2390
26 A-PD	52 A-PD	78 A-PD	2.123	47.92	0.470	0.851	1.193	0.2510
26 A-PD	52 A-PD	78 A-PD	2.099	46.07	0.570	0.760	0.620	0.2249

The initial state of charge of the cell was 76.14 % for all experiments at 20 °C. Afterwards, the cell was applied to constant current discharge (CCD) and constant current charge (CCC) procedures. The battery cell was then charged until it reached the upper voltage limit, corresponding to a 100 % SOC. Discharge from 74.92 % to 46.07 % SOC demonstrated a quasi-linear voltage decrease concerning SOC.

With the intention of understanding the internal resistance impact on heat generation, as one of the principal sources of irreversible heat generation, the internal resistance was determined at different SOC levels using hybrid pulse cycle experiments. The cells' internal resistance changes under a dissimilar SOC, causing the discrepancy in heat generation under the identical working current. The complete procedure for the determination of the internal resistance is described in Figure 3. Various loading patterns were applied to the cell to get the internal resistance.

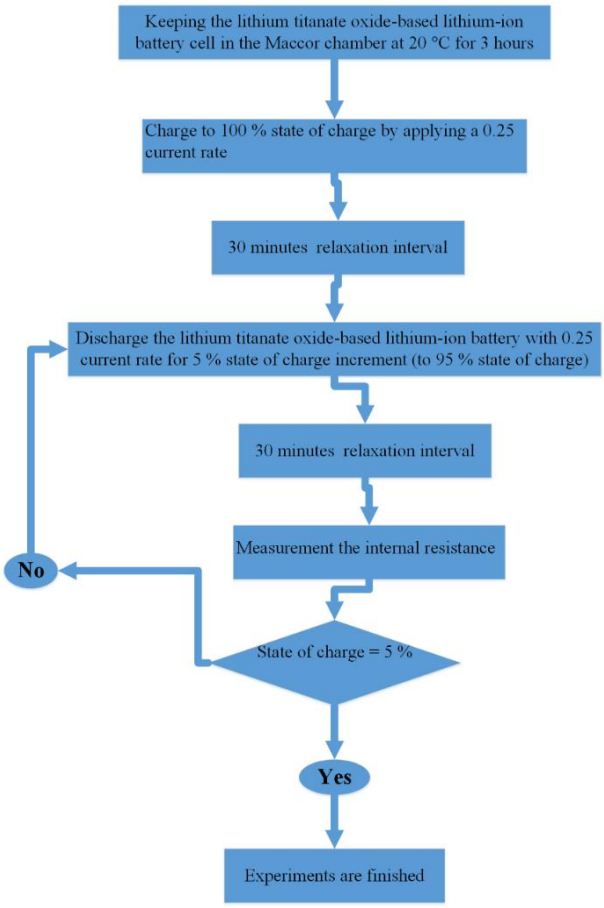

Figure 3. The procedure for measuring the internal resistance.

Heat loss could be estimated by the sum of the quantitative determination of the irreversible and reversible heat sources for LIB. Reversible heat generation of LIB usually is a linear function of current rates, notwithstanding irreversible heat generation of the LIB is a function of current squared [1,43]. Lithium-ion battery internal resistance is one of the principal sources of irreversible heat generation. Besides, it is dependent on the temperature. Open-circuit voltage (OCV) is one of the primary sources of reversible heat generation. Therefore, the determination of internal resistance and open-circuit voltage assists in understanding the thermal behaviour and heat generation of LIB. Figure 4 describes the procedure for measuring the open-circuit voltage.

Results and discussion

Discharge from 74.92% to 46.07% SOC demonstrated a quasi-linear voltage decrease concerning SOC. Figure 5 demonstrates the dependence of the cell's internal resistance on the SOC during discharging. The internal resistance of the LTO-based cell was almost constant, with around 3 ohms at a SOC >40% and increased up to a factor of three at lower SOC levels. It should be noted that 1C corresponds to 13Ah.

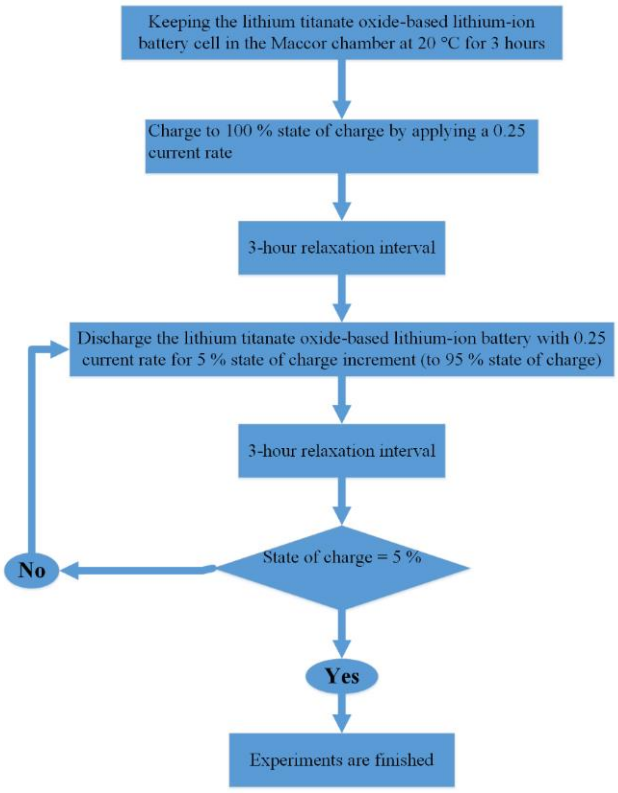

Figure 4. The procedure for measuring the open-circuit voltage.

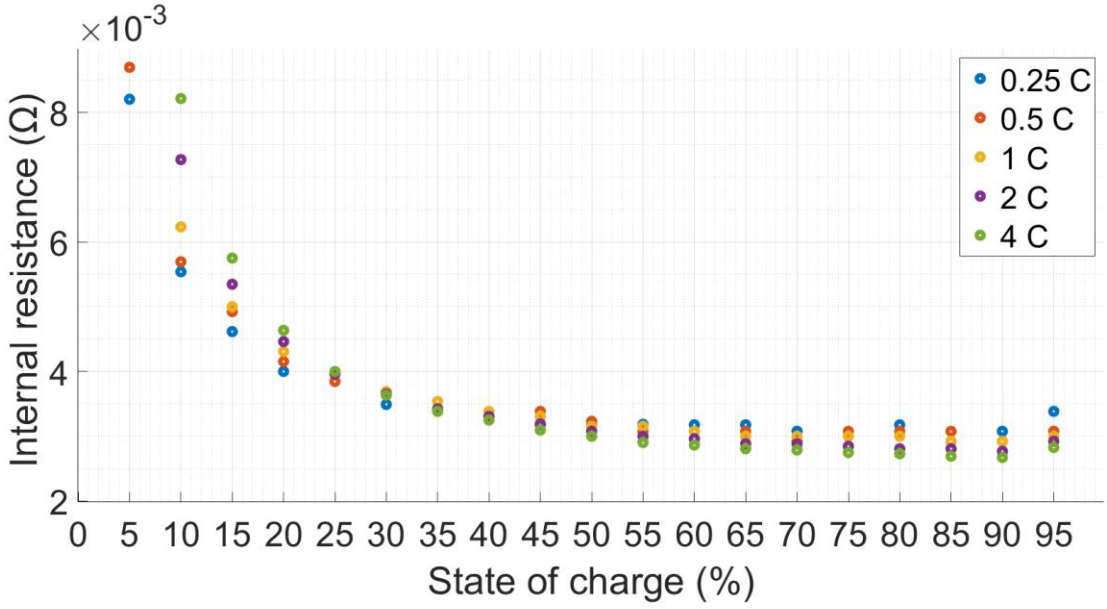

Figure 5. Dependence of the internal resistance (Ω) on the state of charge during different discharging pulses.

Consistent with most of the LTO-based cell parameters, the OCV depends entirely on the working states, including the SOC. The primary purpose of performing OCV measurements was to obtain the correlation between SOC and OCV for discharging conditions and a wide range of SOC levels. Figure 6 shows the dependence of the OCV on the SOC during different discharging pulses.

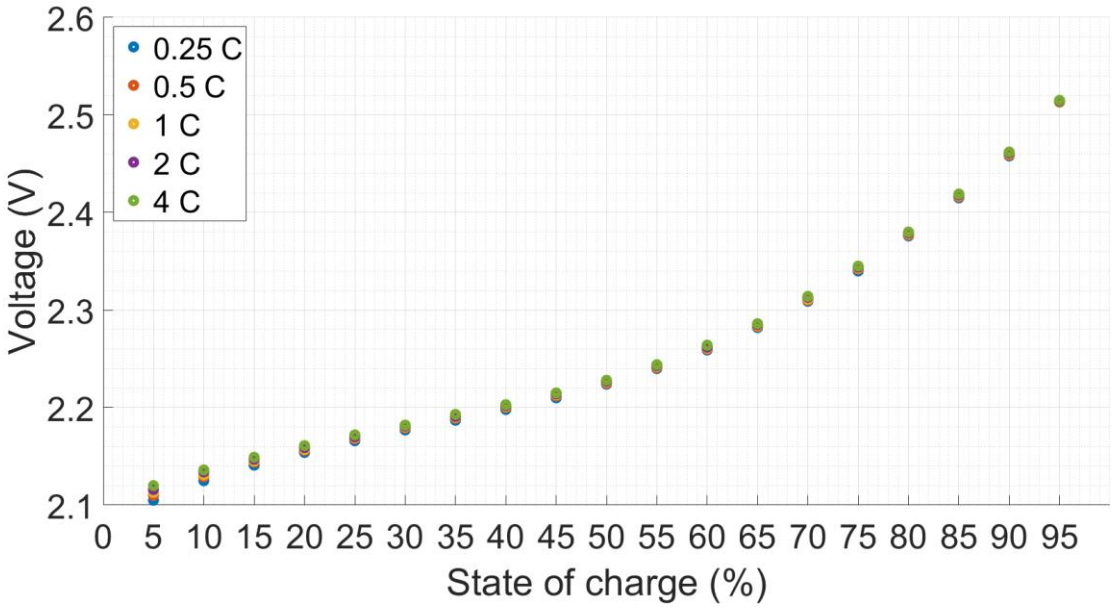

Figure 6. Dependence of the open-circuit voltage (V) on the state of charge during different discharging pulses.

The heat generation curves of the cell that have been determined using the isothermal calorimeter are illustrated in Figure 7(a) and the derived total generated heat is shown in Figure 7(b). Four different current profiles were applied with random and periodic current pulses. Therefore, ten different step time durations were considered for the SOC. Different SOC levels were selected so that cell demonstrated a quasi-linear voltage decrease as a function of SOC. The time-related amalgamation of the heat generation of the cell at different discharge steps, as measured using the isothermal battery calorimeter, corresponds to the total generated heat within a period interval. An overall increasing pattern was seen for the heat generation during discharging, and an overall decreasing pattern was seen for the heat generation during the rest period for each discharge pulse. When the cell was discharged from 74.92% to 68.23% SOC at 20 °C, the heat generation was 0.377 Wh, 0.728 Wh, and 1.002 Wh for 26 A, 52 A, and 78 A step discharge rates, respectively. However, a 1.85% SOC decrease at medium SOC levels corresponds already to 0.57 Wh, 0.76 Wh, and 0.62 Wh heat generation. It can be observed from Fig. 7(b) that the total generated heat curves for the 26 A, 52 A, and 78 A overlap each other until SOC 74.92%,. As the stored energy is discharged more, the three curves start to deviate from each other. In the SOC range from 74.92% to 46.07%, the average heat generation rate during 78 A step discharge cycles was more significant by 0.25 Wh and 0.85 Wh than that observed for the 26 A and 52 A step discharge, respectively. A decrease of 2 % in SOC level causes an increase of 0.4 Wh, 0.776 Wh, 1.064 Wh, and 0.229 Wh in heat generation for Step 26 A, 52 A, 78 A discharge at 20 °C and step 26 A discharge at 30 °C, correspondingly.

It can be concluded from these experimental data that the SOC level change at different SOC points has a different influence on the heat generation rate. The rise in irreversible heat generation at more considerable current rates might be attributable to elevated overpotential. Overpotential resistance decreases with an increasing state of charge level towards the end of discharge.

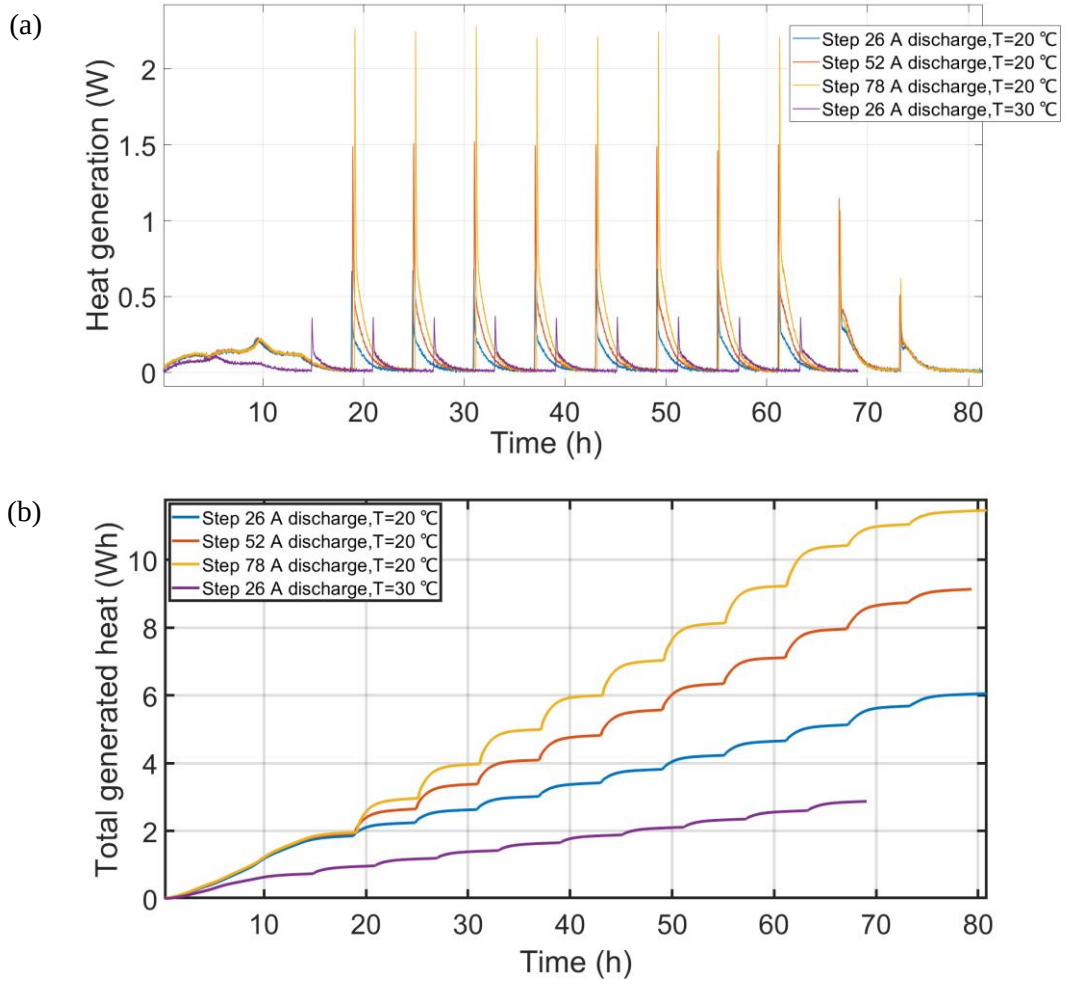

Figure 7. Isothermal calorimeter measurements on the LTO-based cell: (a) Heat generation curves for different current rates (b) Evolution of total generated heat as derived from (a).

The quantity of total generated heat decreases significantly at 30 °C in comparison with the working temperature of 20 °C. It can be inferred that the operating temperature of the LTO-based cell is the most crucial factor affecting heat generation. Notwithstanding, SOC level change could be significant in some SOC points; nonetheless, the impact of irreversible heat and internal resistance is not insignificant.

Open-circuit voltage demonstrated an increasing pattern towards a higher charge state; conversely, internal resistance showed approximately an overall decreasing pattern towards a higher state of charge. Considering the changing pattern of heat generation at different state of charge levels and total generated heat, it can be concluded that internal resistance has a greater influence on heat generation of the LTO-based cell in comparison with open-circuit voltage.

The calorimeter experiments demonstrated that the heat generation rate changed non-monotonically at different SOC levels and increased significantly towards the beginning of discharge. The aforementioned may be explained by the different contributions of the heat of mixing, heat of phase change, and irreversible and reversible heat at different state of charge levels. An overall increasing pattern was observed for the total generated heat of the LTO-based cell throughout the discharge process. Notwithstanding, in the literature, various lithium-ion batteries showed different behaviour in

their heat generation. In ref. [28] heat generation of prismatic LIB was measured, and a decrease in heat generation rate at a depth of discharge of almost 30 % was observed. In addition, an observable secondary plateau in LIB heat generation was recognized for elevated battery working temperatures at a depth of discharge of around 80 %. In ref. [5] heat generation experiments were accomplished in a high-power prismatic cell. The results indicate that entropic heat is endothermic throughout discharge between 60–40% state of charge and exothermic until 80% state of charge. As mentioned above, the change becomes exothermic at an equal and less than 20% state of charge.

Figure 8 shows the surface temperature evolution of the cell. It can be seen that for all the selected locations on the cell's surface, the temperature increases during discharging conditions, which shows that the electrochemical reaction is exothermic throughout the discharge pulses. However, the temperature decreases throughout the rest period. The maximum increase in temperature of the cell for different discharge pulses is proportional to the amount of heat generation.

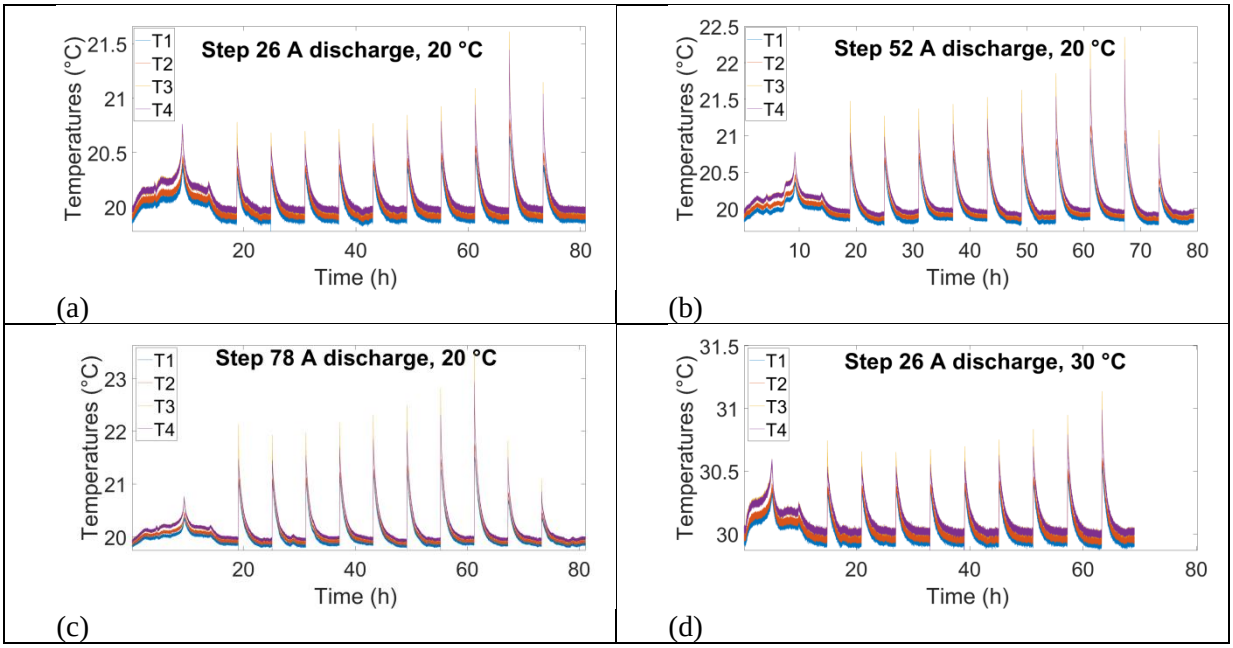

Figure 8. Surface temperature evolution of the LTO-based cell. (a) Step 26 A discharge, 20 °C, (b) Step 52 A discharge, 20 °C, (c) Step 78 A discharge, 20 °C, (d) Step 26 A discharge, 30 °C.

The chemical reactions cause the heat to be stored within the cell. Because the heat dissipation from the cell to the chamber is not large enough, the heat generation increases primarily in the discharge process and is reduced while the overpotential decreases. This phenomenon results in a fast increase in the cell's temperature at the beginning of the discharge process and a subsequent further increase.

Discharge and charge at various current rates exhibited a relatively dissimilar orientation in the temperature profile. During charge and discharge, this turns out to be negligible, as shown by an insignificant variation in the slope of the temperature profile. At different current rates, the most extensive heated parts were located at the neighbouring regions of the tabs, and the temperatures were relatively more considerable in the neighbourhood of the negative tab.

The quantity of irreversible heat, including resistance heat, may turn out to be more significant at a higher current rate. Throughout the 78 A step discharge, the heat generation was remarkably higher than that of the 26 A and 52 A step discharge throughout all the discharge process. The produced heat during each step discharge cycle was not proportional to the amount of SOC decrease. Nevertheless, it

was seen that this relationship might change according to the quantity of step discharge current. The maximum heat generation for 26 A step discharge cycles was from 47.92% SOC to 46.07% SOC, while for both 52 A and 78 A step discharge cycles, it was from 50.23% SOC to 47.92% SOC. The minimum heat generation for 26 A step discharge cycles was from 74.92% to 68.23% SOC, while for 52 A, it was from 62.69% to 58.61% SOC and for 78 A step discharge cycles, it was from 47.92% to 46.07% SOC. At 30°C, discharging from 74.92% to 68.23% SOC, the heat generation was 0.22 Wh for 26 A step discharge rates. The maximum heat generation for 26 A-step discharge cycles was from 50.23% to 47.92% SOC. These changes could be associated with irreversible and reversible heat source parts. These parameters are more significant at the lowest and highest SOC levels. Besides, this might also be related to reversible entropic variations or diffusion limitations as well as the heat of mixing and heat of phase changes.

The lithium titanate oxide battery's heat generation rate and surface temperature distribution depend on different factors, such as the charge or discharge profile, the initial SOC, and the initial temperature. It may also depend on other parameters which were not investigated in this research, such as the LIB construction, design, and chemistry. The pouch cell's temperature distribution turned out to be heterogeneous. It could be inferred that the zone of the largest non-uniformity and temperature is the position where the heat generation is the largest. For the investigated LTO-based pouch cell, the most significant source of heat generation seems to be the tab to the current collector boundary.

The heat generation rate increases faster at the end of discharge than at its beginning. This finding might be due to the reduced terminal voltage while the cell is at a low SOC. In addition, the lithium-ion concentration gradient at the end of discharge might be more significant than at the beginning. The temperature gradient over the cell surface is lower at the beginning of the charge and discharge processes than at their ends.

The evolution of heat loss as a subordinate of the current charge/discharge cycles was determined. This heat flux quantification could be employed for judging the heat transmission of the inner portion of the lithium-ion battery cell. The results of this investigation can be used as supporting benchmark data for correlation to simulation outcomes, accompanied by lithium-ion battery heat generation characteristics to assist in the design and analysis of an efficient thermal management system.

When the operating temperature is 50 °C, the heat generation amount is approximately the same as at 20 °C at the lower current rates and increases comparatively towards significant current rates. The heat generation level increases with the increase of charge and discharge current rates. It is very appealing that there is a heat generation boundary for the investigated cell with individual compounds and materials as a function of operating temperature. Besides, it varies for different current rates.

3. Conclusions

A method using an isothermal calorimeter was introduced to improve the understanding of the thermal phenomena that occur within a LTO-based pouch cell at different operating temperatures and under different operating conditions. Interestingly, the majority of the parameters exhibited an overall increasing or decreasing behaviour towards significant current rates. The isothermal battery calorimeter was employed to study the operational temperature influence on the cells' heat dissipation and efficiency. It was concluded that the current rates were directly proportional to the heat dissipation rate. Using this experimental methodology will assist researchers, cell developers, and producers in deriving essential parameters, including heat generation and lifetime analysis at different current rates in particular operating cases of charge and discharge cycles. It was observed that the discharge and charge current rates substantially impact the thermal behaviour. This study connected the charge and discharge cycles with various current rates to efficiency, peak temperature, and heat generation. An almost linear relationship was revealed between these parameters and the current rate. Constant current discharge pulses at dissimilar current rates were applied. The hybrid pulse power characterization experiment was used to determine the internal resistance at different state of charge levels. The results showed that the reliance of various parameters on the cells' reversible and irreversible heat exhibits substantial changes at different state of charge levels and working conditions.

Nevertheless, their contribution is dissimilar. It was concluded that the heat generation is not negligible even at low rates of pulse discharge current step duration. The heat released during step discharge cycles was not equal in any of the cell's state of charge levels investigated. Total generated heat demonstrated a significant dependence on the SOC level, pulse discharge current step duration, ambient temperature, and discharge rate. Nevertheless, these influential parameters may have a different impact on the heat of mixing, the heat of phase change, and irreversible and reversible heat at different SOC levels. The impact of SOC level on heat generation of the cell turned out to be larger at a lower SOC compared to a higher SOC. It can be concluded that at a high SOC level, the significance of the internal resistance affecting the heat generation is lower than that of the level of SOC change, whereas, at a small SOC level, the working temperature is most critical, followed by internal resistance and SOC level.

The total generated heat for a step current discharge at 78 A increased more than for other currents. A decrease of 6.69 % in SOC level caused an increase of 0.377 Wh, 0.728 Wh, 1.002 Wh, and 0.2249 Wh in heat generation for Step 26 A, 52 A, 78 A discharge at 20 °C and stepped 26 A discharge at 30 °C respectively. Such values and findings can be used at first to assess, examine, and develop LTO-based modules and battery packs. Second, they help to elaborate a much more accurate thermal model of the cell. Third, they are valuable to tailoring thermal management systems by optimizing cooling capacity and sketching cooling routes via the battery packs. Accordingly, this can cause safer operation and a longer lifetime of LIB. This research can contribute to future studies about thermal behaviour and management of LIB.

References

[1] Manikandan B, Yap C, and Balaya P 2017 Towards Understanding Heat Generation Characteristics of Li-Ion Batteries by Calorimetry, Impedance, and Potentiometry Studies, *J. Electrochem. Soc.* **164** no. 12, A2794–A2800

[2] Guldbæk L, Karlsen and Villadsen J 1987 Isothermal reaction calorimeters - I. A literature review, *Chem. Eng. Sci.* **42** no. 5, 1153–1164

[3] Untereker D F 1978 The Use of a Microcalorimeter for Analysis of Load - Dependent Processes Occurring in a Primary Battery, *J. Electrochem. Soc.* **125** no.12, 1907–1912

[4] Tudron F B Dynamic Microcalorimetry: Thermal Effects of Miniature Alkaline Cells Under Load., *J. Geophys. Res.* **79** no. 2, 437–439

[5] Abdul-Quadir Y et al. 2014 Heat generation in high power prismatic Li-ion battery cell with LiMnNiCoO2 cathode material, *Int. J. Energy Res*. **38** no. 11, 1424–1437

[6] Awarke A, Jaeger M, Oezdemir O, and Pischinger S 2012 Thermal analysis of a li-ion battery module under realistic ev operating conditions, *International Journal for Energy Research*, 1099-114

[7] Jeon D H and Baek S M 2011 Thermal modeling of cylindrical lithium ion battery during discharge cycle, *Energy Conversion and Management* **52** 2973-2981.

[8] Kim U S, Shin C B and Kim C S 2008 Effect of electrode configuration on the thermal behavior of a lithium polymer battery *Journal of Power Sources*, 180, 909-916

[9] Shen J, Wang Y, Yu G and Li H, 2020 Thermal Management of Prismatic Lithium-Ion Battery with Minichannel Cold Plate, *J. Energy Eng.* **146** no. 1.

[10] Madani S S, Schaltz E and Kær S K 2018 Study of Temperature Impacts on a Lithium-Ion Battery Thermal Behaviour by Employing Isothermal Calorimeter *ECS Trans.* **87** no.1

[11] Madani S S, Schaltz E and Kær S K 2018 Investigation of the Effect of State-of-Charge and C-Rates on the Heat Loss and Efficiency of a Lithium-Ion Battery *ECS Trans.* **87** no.1, 51–58

[12] Madani S S, Schaltz E and Kær S K 2018 Heat loss measurement of lithium titanate oxide batteries under fast charging conditions by employing isothermal calorimeter *Batteries* **4** no.4, 59

[13] Madani S S, Schaltz E and Kær S K 2018 Thermal Modelling of a Lithium Titanate Oxide Battery *ECS Trans* **87** no.1, 315–326
[14] Madani S S 2020 Experimental Study of the Heat Generation of a Lithium-Ion Battery *ECS Trans.* **99** no.1, 419
[15] Hall F, Touzri F, Wußler S, Buqa H, and Bessler W G 2018 Experimental investigation of the thermal and cycling behavior of a lithium titanate-based lithium-ion pouch cell, *J. Energy Storage*, 17, 109–117
[16] Wu W, Xiao X, and Huang X 2012 The effect of battery design parameters on heat generation and utilization in a Li-ion cell, *Electrochem. Acta*, 83, 227–240.
[17] Chen S C, Wan C C, and Wang Y Y 2005 Thermal analysis of lithium-ion batteries, *J. Power Sources*, **140** no. 1, 111–124
[18] Jeon D H and Baek S M 2011 Thermal modeling of cylindrical lithium ion battery during discharge cycle. *Energy Conversion and Management*, 52, 2973-2981
[19] Kim U S, Shin C B and Kim C S 2008 Effect of electrode configuration on the thermal behavior of a lithium polymer battery *Journal of Power Sources*, 180, 909-916
[20] Yang H and Prakash J 2004 Determination of the Reversible and Irreversible Heats of a LiNi0.8Co0.15Alsub0.05O2/Natural Graphite Cell Using Electrochemical-Calorimetric Technique, *J. Electrochem. Soc.* **151** no. 8, A1222
[21] Kobayashi Y et al. 1999 Electrochemical and calorimetric approach to spinel lithium manganese oxide, *J. Power Sources*, 81–82, 463–466.
[22] Kantharaj R and Marconnet A M 2019 Heat Generation and Thermal Transport in Lithium-Ion Batteries: A Scale-Bridging Perspective, *Nanoscale Microscale Thermophys. Eng.*, **23** no. 2, 128–156
[23] Ma S et al. 2018 Temperature effect and thermal impact in lithium-ion batteries: A review, *Prog. Nat. Sci. Mater. Int.* **28** no. 6, 653–666
[24] Bandhauer T M, Garimella S, and Fuller T F 2011 A Critical Review of Thermal Issues in Lithium-Ion Batteries, *J. Electrochem. Soc.* **158** no. 3
[25] Onda K, Kameyama H, Hanamoto T, and Ito K 2003 Experimental Study on Heat Generation Behavior of Small Lithium-Ion Secondary Batteries, *J. Electrochem. Soc.* **150** no. 3, A285
[26] Bang H, Yang H, Sun Y K, and Prakash J 2005 In Situ Studies of Li[sub x]Mn[sub 2]O[sub 4] and Li[sub x]Al[sub 0.17]Mn[sub 1.83]O[sub 3.97]S[sub 0.03] Cathode by IMC, *J. Electrochem. Soc.* **152** no. 2, A421
[27] Zhang J et al. 2014 Comparison and validation of methods for estimating heat generation rate of large-format lithium-ion batteries, *J. Therm. Anal. Calorim.* **117** no. 1, 447–461
[28] Chen K, Unsworth G, and Li X 2014 Measurements of heat generation in prismatic Li-ion batteries, *J. Power Sources* 261, 28–37
[29] Bandhauer T M, Garimella S and Fuller T F 2014 Temperature-dependent electrochemical heat generation in a commercial lithium-ion battery, *J. Power Sources* 247, 618–628.
[30] Schuster E, Ziebert C, Melcher A, Rohde M, and Seifert H J 2015 Thermal behavior and electrochemical heat generation in a commercial 40 Ah lithium ion pouch cell *J. Power Sources* 286, 580–589
[31] Lin C, Xu S, Li Z, Li B, Chang G and Liu J 2015 Thermal analysis of large-capacity LiFePO4 power batteries for electric vehicles *J. Power Sources* 294, 633–642
[32] Drake S J et al. 2015 Heat generation rate measurement in a Li-ion cell at large C-rates through temperature and heat flux measurements *J. Power Sources* 285, 266–273
[33] Madani S S, Schaltz E and Kær S K 2018 Review of parameter determination for thermal modeling of lithium ion batteries *Batteries*. **4** no.2, 20
[34] Madani S S, Swierczynski M J and Kaer S K 2017 A review of thermal management and safety for lithium ion batteries 2017 *12th International Conference on Ecological Vehicles and Renewable Energies*, EVER 2017, 1-20

[35] Ohzuku T, Ueda A and Yamamoto N 1995 Zero-Strain Insertion Material of Li[Li1/3Ti5/3]O4 for Rechargeable Lithium Cells *Journal of The Electrochemical* **142** no.5, 1431–1435

[36] Yi T F, Jiang L J, Shu J, Yue C B, Zhu R S and Qiao H B 2010 Recent development and application of Li4Ti5O12 as anode material of lithium ion battery *Journal of Physics and Chemistry of Solids* **71**,1236 – 1242